Protein Science (2000), *9*:859–866. Cambridge University Press. Printed in the USA.
Copyright © 2000 The Protein Society

Binding of Zn^{2+} to a Ca^{2+} loop allosterically attenuates the activity of factor VIIa and reduces its affinity for tissue factor

LARS C. PETERSEN,[1] OLE H. OLSEN,[2] LARS S. NIELSEN,[3] PER-OLA FRESKGÅRD,[1] AND EGON PERSSON[1]

[1]Tissue Factor/Factor VII Research, Novo Nordisk A/S, Novo Nordisk Park, DK-2760 Måløv, Denmark
[2]Medicinal Chemistry Research IV, Novo Nordisk A/S, Novo Nordisk Park, DK-2760 Måløv, Denmark
[3]Molecular Genetics, Novo Nordisk A/S, Novo Alle 1, DK-2880 Bagsværd, Denmark

(RECEIVED October 26, 1999; FINAL REVISION February 28, 2000; ACCEPTED March 10, 2000)

Abstract

The protease domain of coagulation factor VIIa (FVIIa) is homologous to trypsin with a similar active site architecture. The catalytic function of FVIIa is regulated by allosteric modulations induced by binding of divalent metal ions and the cofactor tissue factor (TF). To further elucidate the mechanisms behind these transformations, the effects of Zn^{2+} binding to FVIIa in the free form and in complex with TF were investigated. Equilibrium dialysis suggested that two Zn^{2+} bind with high affinity to FVIIa outside the N-terminal γ-carboxyglutamic acid (Gla) domain. Binding of Zn^{2+} to FVIIa, which was influenced by the presence of Ca^{2+}, resulted in decreased amidolytic activity and slightly reduced affinity for TF. After binding to TF, FVIIa was less susceptible to zinc inhibition. Alanine substitutions for either of two histidine residues unique for FVIIa, His216, and His257, produced FVIIa variants with decreased sensitivity to Zn^{2+} inhibition. A search for putative Zn^{2+} binding sites in the crystal structure of the FVIIa protease domain was performed by Grid calculations. We identified a pair of Zn^{2+} binding sites in the Glu210–Glu220 Ca^{2+} binding loop adjacent to the so-called activation domain canonical to serine proteases. Based on our results, we propose a model that describes the conformational changes underlying the Zn^{2+}-mediated allosteric down-regulation of FVIIa's activity.

Keywords: calcium loop; factor VIIa; tissue factor; Zn^{2+} binding; zinc inhibition

Nutritional zinc deficiency is associated with bleeding and defective platelet aggregation, suggesting an essential role in the hemostatic process for this ion (Gordon et al., 1982). Platelets accumulate Zn^{2+}, mainly in the cytoplasm and α-granules, to levels 30–60-fold higher than the normal plasma level of about 17 μM. Considerable amounts are released upon platelet stimulation (Gorodetsky et al., 1993), presumably leading to high local concentrations at sites of vascular injury. Zn^{2+} enhances the activation of the intrinsic coagulation system by increasing the binding of high molecular weight kininogen and factor XII to negatively charged surfaces (Bernardo et al., 1993a, 1993b), and by affecting the activations of factor XII and prekallikrein (Shimada et al., 1987; Shore et al., 1987; Schousboe, 1990). In contrast, Zn^{2+} has an inhibitory effect on the extrinsic system by a specific attenuation of FVIIa and FVIIa/tissue factor (TF) activity, an effect not observed with other vitamin K-dependent coagulation factors (Pedersen et al., 1991). Another peculiarity of FVIIa compared to other serine proteases is the property of its active site to obey cofactor-induced allosteric regulations as indicated by a profound stimulation of amidolytic activity induced by TF and calcium ions (Pedersen et al., 1990; Higashi et al., 1992). This is presumably linked to the propensity of free FVIIa to exist primarily in an inactive conformation. Compared to in the FVIIa/TF complex, the amino-terminal Ile153{16} (chymotrypsinogen numbering in curly brackets throughout) in free FVIIa is more susceptible to chemical modification, and the lack of a salt bridge with Asp343{194} (adjacent to the active site Ser) is probably the reason for the zymogen-like nature of free FVIIa (Higashi et al., 1994). How binding of TF to FVIIa accomplishes to establish the Ile153–Asp343 salt bridge is a matter of intense investigation. Alanine scanning (Dickinson et al., 1996) and crystallographic studies comparing the structures of FVIIa/TF (Banner et al., 1996; Zhang et al., 1999) and free FVIIa (Pike et al., 1999) have suggested that TF activates FVIIa through stabilization of the so-called activation domain (Huber & Bode, 1978). Binding

Reprint requests to: Lars C. Petersen, Tissue Factor/Factor VII Research, Novo Nordisk A/S, Novo Nordisk Park, DK-2760 Måløv, Denmark; e-mail: lcp@novo.dk.

of TF to FVIIa, more precisely the insertion of Met306{164} into a small surface cavity on TF, appears to induce an α-helical structure comprising residues 307{165}–312{170} that restricts the flexibility of the following loop, and in turn, stabilizes the activation domain that allows insertion of Ile153{16} (Pike et al., 1999). Implications of the calcium binding loop, Glu210{70}–Glu220{80}, in the allosteric regulation of FVIIa activity have also been indicated. There is a marked Ca^{2+} dependency of FVIIa's amidolytic activity (Pedersen et al., 1990), which is affected by replacements of calcium loop residues (Wildgoose et al., 1993; Dickinson et al., 1996). Moreover, Glu296{154} at the interface between the calcium loop and the activation domain has been shown to be involved in the regulation of FVIIa's catalytic function (Shobe et al., 1999). Thus, conformational changes act as switches on opposite sides of the activation domain to enhance the activity of the catalytic center of FVIIa (Fig. 1). The specific inhibition of FVIIa by Zn^{2+} and the competition between Zn^{2+} inhibition and Ca^{2+} stimulation (Pedersen et al., 1991; Petersen et al., 1994) is suggestive of Zn^{2+} binding to the Ca^{2+} site in the protease domain. An understanding of the mechanism behind zinc inhibition might shed light on how occupation of this site is linked to the catalytic function of FVIIa. Here we report on the number, locations, and effects of Zn^{2+} bound to FVIIa and present a model of how the Zn^{2+}-induced conformational change propagates to affect the active site.

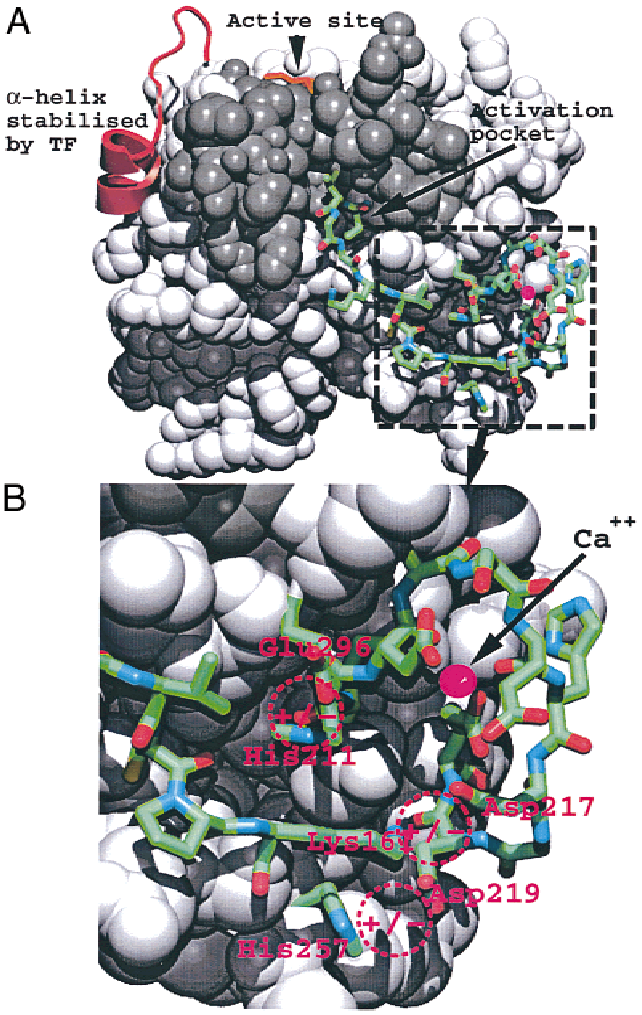

Fig. 1. The protease domain of FVIIa with a close-up of the calcium-binding loop. **A:** The majority of the domain (PDB code 1dan) is shown in space-filling representation. The active site D-Phe-Phe-Arg inhibitor (orange), the N-terminal region Ile153–Lys161{16–24}, the calcium loop Glu210–Glu220{70–80}, Glu296{154}, and His257{117} are drawn in stick representation. The calcium ion is shown as a magenta sphere. The serine protease activation domain (see text for definition) is colored gray. The region encompassing Thr306–Pro321{164–170I} is schematically shown as the local secondary structure (red). **B:** The area around the calcium loop is shown in more detail. The position of three potential salt bridges, Glu296–His211{154–71}, His257–Asp219{117–79}, and Lys161–Asp217/Asp219{24–77/79} possibly connecting the calcium loop and the activation domain are marked with dotted circles.

Results

Binding of Zn^{2+} to FVIIa and concomitant inhibition of amidolytic activity

Zinc ions are known to bind to the Gla domain of vitamin K-dependent coagulation factors, but only to inhibit the catalytic activity of one of these proteins, FVIIa (Pedersen et al., 1991). It was also shown that zinc inhibition of FVIIa's amidolytic activity is unaffected by deletion of its Gla domain, i.e., FVIIa and des(1–44)–FVIIa were similarly affected, indicating that binding sites outside this domain are responsible for the inhibitory effect. It was therefore of interest to characterize the binding of Zn^{2+} to des(1–44)–FVIIa in further detail. Equilibrium dialysis measurements indicated that des(1–44)–FVIIa contains three or possibly four binding sites for Zn^{2+}, two of relatively higher affinity (Fig. 2A). The binding of Zn^{2+} to at least one of the high-affinity sites in des(1–44)–FVIIa appeared to be impaired by the presence of 5 mM Ca^{2+}. This indicates that Zn^{2+} competes with Ca^{2+} for at least one site in des(1–44)–FVIIa. This is in accordance with a previous report showing decreased Zn^{2+} inhibition of FVIIa's amidolytic activity with increasing Ca^{2+} concentration (Pedersen et al., 1991; Petersen et al., 1994).

The effect of Zn^{2+} on the amidolytic activity of FVIIa and FVIIa/$TF_{1–219}$ was investigated in the presence of 1 mM $CaCl_2$ (results not shown). The data were in agreement with a previous report, with more potent inhibition of free FVIIa (Pedersen et al., 1991). Half-maximal inhibition of free and TF-bound FVIIa were achieved at 20 and 60 μM, respectively. The results also suggested a competition between Ca^{2+} and Zn^{2+} for a common site(s). A detailed analysis of the inhibitory effect of Zn^{2+} was performed to try to correlate the effect on FVIIa's activity with the direct Zn^{2+} binding data. The inhibition data obtained with free FVIIa were best described by a two-site model (Fig. 2B). Taken together, the results in Figure 2 strongly suggest that the two high-affinity sites deduced from the equilibrium dialysis experiment are responsible for the inhibitory effect of Zn^{2+}.

Effect of Zn^{2+} on binding of TF to FVIIa

The above results revealed that binding of $TF_{1–219}$ to FVIIa resulted in a decreased inhibitory effect of Zn^{2+}. The possibility that binding of Zn^{2+} to FVIIa might impede binding to TF was examined. Figure 3A shows that binding of FVIIa to immobilized $TF_{1–219}$ was decreased by Zn^{2+}. The addition of 0.3 mM $ZnCl_2$ resulted in an increase in K_d from ~5 to 25 nM. The effect occurred with a

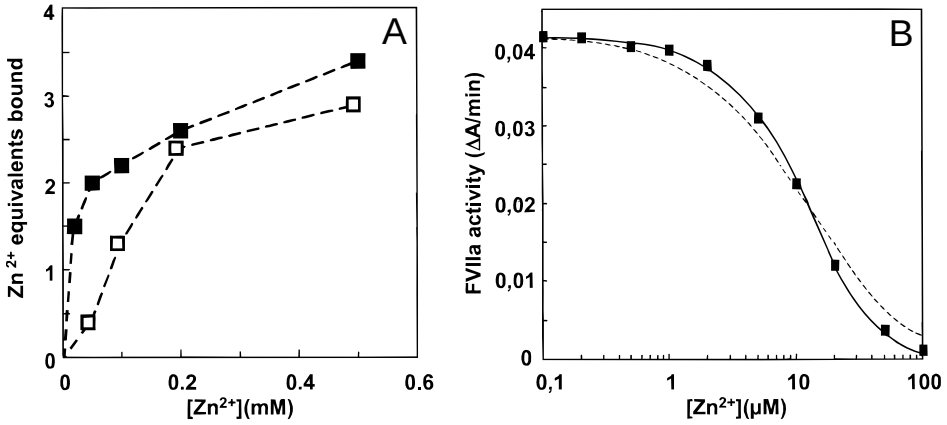

Fig. 2. Equilibrium dialysis measurements of Zn^{2+} binding to des(1–44)–FVIIa and the Zn^{2+} effects on FVIIa amidolytic activity. The number of Zn^{2+} bound to des(1–44)–FVIIa in the presence (□) and absence (■) of 5 mM $CaCl_2$ is shown as a function of the zinc concentration (**A**). The residual FVIIa activity at different Zn^{2+} concentrations up to 0.1 mM was fitted to two-site ($v_i = v_0/(1 + [Zn]/K_i + [Zn]^2/K_i^2)$, solid curve) and one-site ($v_i = v_0/(1 + [Zn]/K_i)$, dashed curve) models, where v_i and v_0 are the activities in the presence and absence of Zn^{2+}, respectively (**B**).

midpoint at about 20 μM Zn^{2+} (Fig. 3B). It is noteworthy that the dissociation was only partial such that further displacement of FVIIa was not obtained when the Zn^{2+} concentration was elevated beyond 0.1 mM.

Previous measurements of FVIIa binding to TF by surface plasmon resonance (Head et al., 1997) showed that Zn^{2+} could not replace Ca^{2+} as a mandatory cofactor for complex formation. When we measured the effect of Zn^{2+} on binding of FVIIa to $TF_{1–219}$ in the presence of 1 mM Ca^{2+} by this technique we found that the K_d increased with increasing concentration of Zn^{2+} (Table 1). The K_d increased threefold in the presence of 0.5 mM $ZnCl_2$, essentially due to an effect on k_{on}. Again, complete prevention of binding was not obtained.

Effect of Zn^{2+} on FFR-chloromethyl ketone alkylation and carbamylation of FVIIa

To distinguish between a general inactivation and a specific effect on the active site geometry of FVIIa we tested the effect of zinc and calcium ions on FFR-chloromethyl ketone alkylation of FVIIa. Figure 4A shows that FVIIa inactivation by FFR-chloromethyl ketone was strongly attenuated by 0.2 mM Zn^{2+}, suggesting an effect on the active site configuration.

Carbamylation has been shown to inactivate FVIIa mainly by modification of the N-terminal Ile153{16} (Higashi et al., 1994). Contrary to chloromethyl ketone alkylation, Zn^{2+} did not affect FVIIa inactivation by carbamylation (Fig. 4B) although the bind-

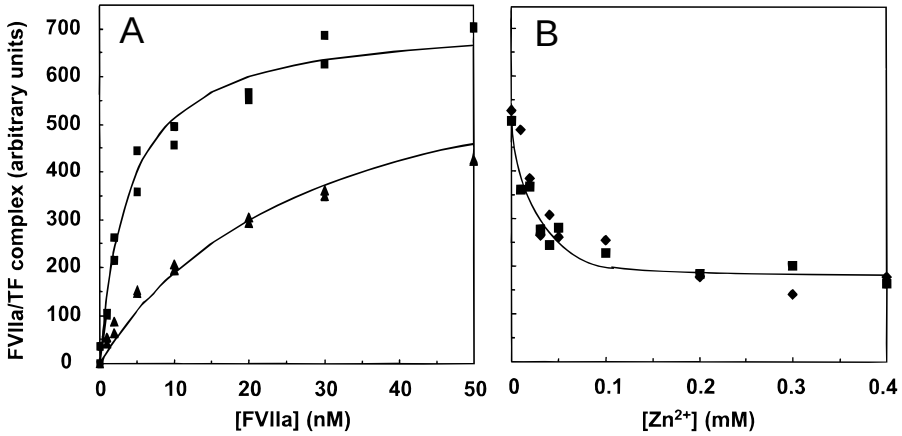

Fig. 3. Effect of Zn^{2+} on the binding of FVIIa to $TF_{1–219}$. **A:** Binding of FVIIa to immobilized TF was measured by incubation of FVIIa in TF-coated wells for 60 min at 25 °C in the absence (■) or presence (▲) of 0.3 mM $ZnCl_2$. **B:** Binding was also measured by incubation of 10 nM FVIIa in TF-coated wells at various concentrations of $ZnCl_2$ (♦ and ■ represent separate experiments). Following incubation and washing, the activity of bound FVIIa was determined by addition of 0.4 mM S-2288 and measurement of the increase in absorbance at 405 nm.

Table 1. *Effect of Zn^{2+} on the binding of factor VIIa to tissue factor*

$[Zn^{2+}]$ (mM)	k_{on}[a] (10^5 $M^{-1}s^{-1}$)	k_{off} ($10^{-3}s^{-1}$)	K_d (nM)
0	3.8	1.4	3.7
0.1	2.9	1.2	4.1
0.2	2.3	1.2	5.2
0.5	1.4	1.4	10

[a] k_{on} and k_{off} were calculated using the BIAevaluation 2.1 software supplied with the Biacore instrument. K_d equals k_{off}/k_{on}.

ing of $TF_{1–219}$ clearly protected FVIIa from inactivation as previously shown (Higashi et al., 1994). This suggests that, in contrast to TF, Zn^{2+} exerts an effect on FVIIa activity by a mechanism that does not involve a change in Ile153{16} exposure.

Effects of site-directed mutagenesis of His216{76} and His257{117} on Zn^{2+} inhibition

Sequence alignment of FVIIa, factor IX, and factor X shows that Lys161{24}, His216{76}, Asp219{79}, His257{117}, and Glu296{154} are unique for FVII. Furthermore, inspection of the crystal structure of FVIIa (Fig. 1) shows two potential salt bridges, Glu296{154}–His211{71} and His257{117}–Asp219{79}, which can mediate contact between the calcium loop and the activation domain. It also reveals a third salt bridge, Lys161{24}–Asp217{77}/Asp219{79}, which stabilizes the N-terminus of the protease domain. This, and experiments showing that Ala substitutions for Lys161{24}, Asp219{79}, and Glu296{154} resulted in loss of proteolytic function, led us to the hypothesis that His216{76} and His257{117} might be ligands to Zn^{2+} allowing it to specifically inhibit FVIIa's activity.

To test this hypothesis, we produced three FVIIa variants: His216Ala–FVIIa, His257Ala–FVIIa, and His216Ala,His257Ala–FVIIa. Substituting Ala for His216{76}, His257{117}, or both residues was without a significant effect on the Ca^{2+} dependence of the amidolytic activity of the resulting FVIIa variants (Fig. 5A). However, the substitutions clearly decreased the sensitivity to Zn^{2+} (Fig. 5B). The double mutant exhibited an additive effect of the individual mutations with half-maximal inhibition at 0.1 mM, fivefold higher than wild-type FVIIa (IC_{50} = 0.02 mM). Intermediate effects were obtained when replacing His216{76} or His257{117} alone.

Identification of putative Zn^{2+}-binding sites in des(1–44)–FVIIa

Because Ala substitutions of residues in the calcium-binding loop of the protease domain resulted in a decreased zinc ion inhibition without affecting the Ca^{2+} stimulation, we probed a model of des(1–44)–FVIIa, based on the crystal structure of the FVIIa/TF complex (Banner et al., 1996), with a zinc ion in an attempt to identify putative binding sites outside the Gla region. Probing this model with a Ca^{2+} probe resulted in the identification of one high-affinity site located in the protease domain exactly in the position where Ca^{2+} was identified in the crystal structure (not shown). A similar procedure performed with a Zn^{2+} probe identified a site in the same region as the calcium site (Fig. 6A). In contrast to the Ca^{2+} probe, the Zn^{2+} probe identified a low interaction energy contour that spanned a rather wide region and guided the positioning of two zinc sites separated by 3.8 Å. The distance between the two zinc ions is quite small, but similar distances have been observed in the X-ray structures of a variety of Zn^{2+}-binding proteins (Libscomb & Strater, 1996). Refinement of the structure surrounding the proposed zinc-binding motif by energy minimization led to the structure shown in Figure 6B. Each Zn^{2+} is hexa-coordinated in a geometry best described as an octahedron. The two Zn^{2+} are bidentately bridged by Glu215{75}. Other ligands to Zn_1 are the carboxylates

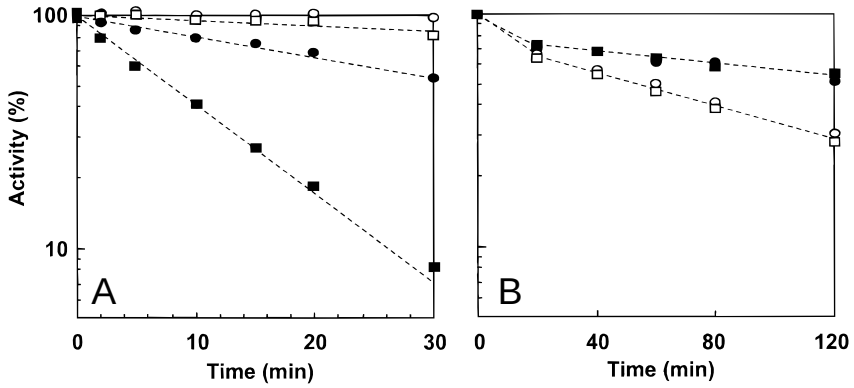

Fig. 4. Effect of Zn^{2+} on the inactivation of FVIIa by FFR-chloromethyl ketone alkylation and carbamylation. **A:** The residual activity of FVIIa (1 μM, open symbols) after incubation with 6 μM FFR chloromethyl ketone and that of FVIIa (40 nM) together with $TF_{1–219}$ (200 nM, filled symbols) after incubation with 120 nM FFR chloromethyl ketone in the absence (□, ■) or presence (○, ●) of 0.2 mM $ZnCl_2$ are shown. **B:** The activity of FVIIa (1 μM, open symbols) and FVIIa (200 nM) together with $TF_{1–219}$ (1 μM, filled symbols) after incubation with 0.2 M KNCO at 37 °C in the absence (□, ■) or presence (○, ●) of 0.2 mM $ZnCl_2$ are shown. In both **A** and **B**, samples were withdrawn at various times and residual amidolytic activity was measured.

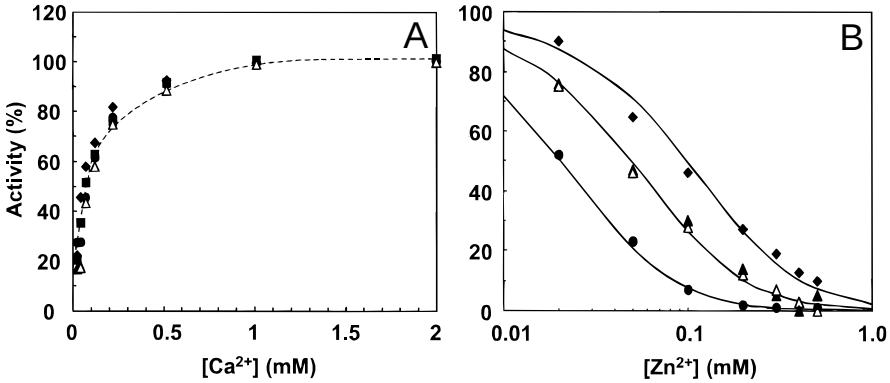

Fig. 5. Effects of Ca^{2+} and Zn^{2+} on the amidolytic activity of His216Ala,His257Ala and His216Ala,His257Ala variants of FVIIa. **A:** The amidolytic activities of 10 nM FVIIa (●), His216Ala–FVIIa (▲), His257Ala–FVIIa (△), and His216Ala,His257Ala–FVIIa (♦) in the presence of 100 nM $TF_{1–219}$ are shown at various concentrations of Ca^{2+}. **B:** The activities of the same variants at a concentration of 100 nM in the absence of TF at various Zn^{2+} concentrations are shown (in the presence of 1 mM $CaCl_2$).

of Glu220{80}, Asp212{72}, and the backbone carbonyls of Asp212{72}, Leu313{Leu73}, and Glu215{75}. Ligands to Zn_2 are the carboxylates of Glu210{70}, Glu215{75}, Asp217{77}, and Glu220{80}. The salt bridge Lys161{24}–Asp217{77}/Asp219{79} is weakened by Zn^{2+} binding. The distance from Lys161{24} to Asp217{77} increased from 2.4 to 3.9 Å, and the distance from Lys161{24} to Asp219{79} increased from 2.8 to 5.4 Å.

The results obtained when His216{76} and His257{117} in FVIIa were replaced with Ala suggested that these residues might be involved in a more direct interaction with Zn^{2+}. Considering this and the prominent weakening of the Lys161{24}–Asp219{79} salt bridge in the above scenario led us to explore a second scenario in which the salt bridge was broken by rotating the side chain of Lys161{24} (using the rotamer library of Ponders, Quanta). Reprobing with Zn^{2+} again identified two possible binding sites. One site (Zn_1) was close to the high-affinity calcium site as before, whereas the other site (Zn_2) was placed in a narrow energy contour close to the basic nitrogen of Lys161{24} (not shown). This structure allows His211{71} and His257{117} to change conformation and become ligands for Zn_2. Manual rotation of the histidines to

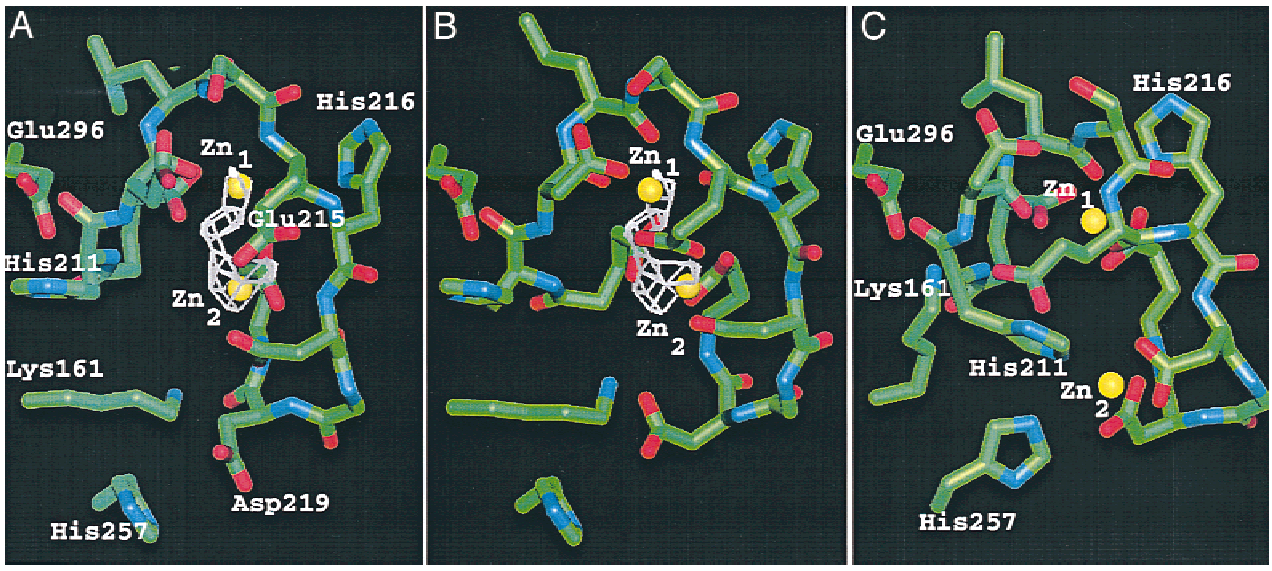

Fig. 6. Putative Zn^{2+} binding sites in the protease domain. The calcium loop residues Glu210–Glu220{70–80}, and the side chains Lys161{24}, Glu296{154}, and His257{117} are shown in stick representation. Amino acid side chains unique for FVIIa are labeled. **A:** Energy contours at −3.0 kcal/mol for a zinc probe interacting with the X-ray structure of FVIIa (Banner et al., 1996) as a white grid with the zinc ions placed within this grid shown as yellow spheres are shown. **B:** The structure after refinement by means of energy minimization of the model in **A** are shown. The zinc ions move only slightly and are still within the grid obtained in the probing. The structure in **C** was obtained after adjustments of side chains in **B** (reorientation of Lys161{24}, repositioning of Zn_2, and final reorientation of His211{71} and His257{117}) followed by energy minimization. The two zinc ions have a variety of ligands in particular from side chains unique for FVIIa.

ligand Zn_2 followed by energy minimization resulted in the structure shown in Figure 6C. Compared to the previous scenario, the distance between the two zinc ions has increased further to 6.1 Å, and several ligands have been replaced. The carboxylates of Glu210{70} and Glu220{80} and the carbonyls of Asp212{72} and Leu213{Leu73} are ligands to Zn_1. Notably, His216{76} is now in a position to interact with Zn_1. The carboxylates of Asp217{77} and Asp219{79} and the imidazoles of His211{71} and His257{117} are ligands to Zn_2.

Discussion

Specific internal proteolytic cleavage normally converts serine protease zymogens into their fully active enzyme forms. The catalytic center is established when the N-terminus produced by this cleavage is inserted into the protease domain, forming a salt bridge with the carboxyl group of an Asp residue adjacent to the active site Ser. FVIIa is an exception to this rule because it attains only a few percent of its maximal activity upon cleavage of the Arg152{15}–Ile153{16} peptide bond and requires binding of Ca^{2+} and TF for full activity. An incomplete insertion of the N-terminus may explain its apparent latency and there appears to be a temperature-dependent equilibrium between an active and an inactive, zymogen-like FVIIa conformation (Higashi et al., 1994; Petersen et al., 1999). A multitude of data now supports the notion that this equilibrium is also affected by binding of Ca^{2+}, TF, and active site inhibitors (Higashi et al., 1994, 1996; Dickinson & Ruf, 1997; Higashi & Iwanaga, 1998; Freskgård et al., 1998; Ruf & Dickinson, 1998). It has been inferred that FVIIa is locked in the active conformation by cross-linking to TF (Miyata et al., 1995). The present work suggests that Zn^{2+} inhibits the activity of FVIIa by specific binding to the Ca^{2+}-binding loop (residues 210{70}–220{80}) joining the β4 and β5 strands of the serine protease domain (Figs. 1, 6) resulting in destabilization of the so-called activation domain.

Equilibrium binding and inhibition studies suggest that FVIIa binds two Zn^{2+} outside the Gla domain with relatively high affinity resulting in inhibition of the enzymatic activity (Fig. 2). Moreover, the residual activity was better described by a two-site model (Fig. 2B), suggesting that occupation of two high-affinity sites is responsible for the inhibition. The studies of the His mutants (Fig. 5) further points to the Ca^{2+}-binding loop in the protease domain as being the region binding Zn^{2+}. Computer modeling indeed confirmed this notion and localized a putative pair of Zn^{2+} sites in the Ca^{2+}-binding surface loop in the protease domain. The search with a zinc probe did not reveal any high affinity sites close to the active site His193{57}, which, based on the inhibitory effect, was suggested by Pedersen et al. (1990) as a putative location for zinc binding. Energy minimization led to two different models for binding of the zinc ions to residues in this loop. In one scenario, the present model suggests that the two Zn^{2+} ions are liganded exclusively to carboxylates and carbonyls, whereas in another scenario three histidines (His216{76}, His211{71}, and His257{117}) are involved as ligands (Fig. 6). Interestingly, sequence alignment of FVIIa, factor IXa, and factor Xa shows that a number of Zn^{2+} ligands, Lys161{24}, His216{76}, Asp219{79}, His257{117}, and Glu296{154}, are unique for FVIIa, and only FVIIa is inhibited by Zn^{2+}.

In both cases the existence of a close overlap between the Ca^{2+} binding site and one of the Zn^{2+} sites (Zn_1) was predicted, suggesting a competition between the two ions for several ligands. Overlapping Zn^{2+} and Ca^{2+} high-affinity sites in the protease domain provides a plausible explanation for experimental findings that the inhibitory effect of Zn^{2+} was partly reversed by Ca^{2+}. The antagonistic action of the two ions on FVIIa activity further suggests that the active FVIIa conformation is destabilized by binding of the two Zn^{2+}. This is corroborated by the reduced accessibility of the active site to the active site inhibitor (Fig. 4A). Binding of Ca^{2+} to the Glu210{70}–Glu220{80} loop, as well as binding of TF to residues 306–309{164–167}, contributes to stabilization of the activation domain (Fig. 1), and both events are presumably required for optimal insertion of the amino terminal Ile153{16} into the activation pocket. We propose that the stabilizing effect of Ca^{2+} binding is exerted via two salt bridges, Glu296{154}–His211{71}, and His257{117}–Asp219{79}, which facilitate contact between the Ca^{2+} loop and the activation domain, and by a third salt bridge, Lys161{24}–Asp217{77}/Asp219{79}, which stabilizes the insertion of the amino terminal Ile153{16} into the activation pocket. Both models described in Figure 6 indicate that occupation of the Zn^{2+} sites interfere with the Lys161{24}–Asp217{77}/Asp219{79} salt bridge. In the first scenario, energy calculations resulted in a marked weakening of the interaction, whereas in the second scenario manual disruption of the His211{71}/Glu296{154} salt bridge and subsequent energy calculations resulted in a structure where also the Glu296{154}–His211{71} and His257{117}–Asp219{79} salt bridges were broken and new interactions established. The importance of Lys161{24}, Asp219{79}, and Glu296{154} for the proteolytic function of FVIIa has been demonstrated by alanine scanning (Dickinson et al., 1996). However, the carbamylation experiment shown in Figure 4B indicates that a weakening of the salt bridge between Lys161{24} and Asp217{77}/Asp219{79} does not influence the insertion of the N-terminal Ile153{16}. This observation suggests that the proposed Zn^{2+}-induced conformational change affects the active site through the activation domain. Glu296{154} also appears to allosterically influence the catalytic site, and an Ala replacement in this position results in suboptimal amidolytic activity (Shobe et al., 1999). The finding of the present study that substitution of Ala for His216{76} or His257{117} decreased Zn^{2+} inhibition (Fig. 5) clearly supports a mechanism involving these residues as outlined by the model shown in Figure 6C. It is also possible that there is an equilibrium between this conformation and that shown in Figure 6B, which might explain why replacement of both His216{76} and His257{117} does not completely abolish zinc inhibition.

The model depicted in Figure 6 may involve a fairly complex situation in terms of sequential occupation of the two Zn^{2+} sites. Occupation of the Zn_1 site occurs with the highest gain in free energy, but at the same time binding to this site is subject to Ca^{2+} competition. In itself, binding of Zn^{2+} to the Zn_1 site appears not to produce a major conformational change and may therefore not lead to the observed inhibition. However, binding of Zn^{2+} to the Zn_1 site appears to be a prerequisite for binding of Zn^{2+} to the Zn_2 site, implicating cooperative binding to the two sites. Occupation of Zn_2 may subsequently generate the conformational changes associated with functional consequences transmitted as described.

In a previous communication (Pike et al., 1999), we proposed that TF binding to Met306{164} and the resulting stabilization of the 307{165}–312{170} helix supports one side of the activation domain. We now propose that unique salt bridges connecting another part of the activation domain with the 210{70}–220{80} loop are important for the transmission of effects on FVIIa activity

induced by Ca^{2+} and Zn^{2+} binding. The carbamylation experiments (Fig. 4B) indicate that the Zn^{2+}-induced conformational changes do not affect the exposure of Ile153{16}, but influence the active site architecture through the activation domain.

The inhibitory effect of Zn^{2+} on FVIIa's activity contrasts the stimulatory effect on FXII and prekallikrein activation. Hence, an enhancement of the intrinsic coagulation pathway appears to be counteracted by an opposite effect on the extrinsic pathway. A cellular release of Zn^{2+} at sites of injury might therefore function as a local physiological regulator of the coagulation process. An understanding of the physiological role of Zn^{2+} in this context requires further investigation.

Materials and methods

Proteins

Human recombinant FVIIa was expressed and purified as previously described (Thim et al., 1988; Persson & Nielsen, 1996). The wild-type FVII expression plasmid, pLN174, contains the FVII cDNA driven by a mouse metallothionein promoter and as a selectable marker dihydrofolate reductase driven by an SV40 promoter. Three His to Ala mutants were prepared using this plasmid as a template by a modified version of inverse polymerase chain reaction (Du et al., 1995). The His257Ala–FVII mutant was constructed using the primers: CTCACTGACGCTGTGGTACC CCTCTGCCTGCCC and GGGTACCACAGCGTCAGTGAGG ACCACGGGCTG, thus introducing a silent AflII site for easy recognition of mutants. His216Ala–FVII was constructed using the primers: GAGCACGACTTAAGCGAGGCCGACGGGGATGAG CAGAGC and ATCCCCGTCGGCCTCGCTTAAGTCGTGCT CGCCCAGCAC similarly introducing a KpnI site. The double mutant His216Ala,His257Ala–FVII was constructed using His216Ala–FVII as a template using the two latter primers. The mutated cDNAs were verified by sequencing. BHK cells (ATCC CRL 1632) were transfected with these constructs using the Qiafect transfection procedure (Qiagen Inc., Chatsworth, California). Selection and production of FVIIa protein were performed as described (Persson & Nielsen, 1996). Des(1–44)–FVIIa was prepared by cathepsin G-mediated cleavage of FVIIa as described (Nicolaisen et al., 1992). Recombinant $TF_{1–219}$ was expressed in *Escherichia coli* and purified as described (Freskgård et al., 1996).

Amidolytic activity measurements

FVIIa and His → Ala mutants alone at a concentration of 100 nM or together with $TF_{1–219}$ (100 nM) at a concentration of 10 nM were incubated with various concentrations of $ZnCl_2$ at 25 °C in 50 mM HEPES, 100 mM NaCl, 1 mM $CaCl_2$, 0.02% Tween 80, pH 7.4, and the activity was measured at 405 nm after addition of 0.4 mM S-2288 substrate (Chromogenix, Mölndal, Sweden).

Measurements of FVIIa binding to immobilized $TF_{1–219}$ by surface plasmon resonance

Measurements of FVIIa binding to $TF_{1–219}$ were performed in a Biacore instrument (Biacore AB, Uppsala, Sweden) as described (Sørensen et al., 1997). $TF_{1–219}$ was immobilization on sensor chip CM5 (research grade).

Measurement of FVIIa binding to immobilized $TF_{1–219}$ by activity measurements

$TF_{1–219}$ was immobilized on Protein Link 96-well plates (Xiqon, Vedbæk, Denmark) by incubating 100 μL of 1 μg/mL $TF_{1–219}$ in 0.1 M $NaHCO_3$, pH 9–10, overnight at 4 °C. The wells were washed three times with buffer A (50 mM HEPES, 100 mM NaCl, 1 mM $CaCl_2$, 0.05% Tween 20, pH 7.4) and subsequently incubated for 20 min with FVIIa (0–50 nM) in buffer A in the presence or absence of 0.3 mM $ZnCl_2$. The wells were washed three times with buffer A, and the amidolytic activity of bound FVIIa was measured with 0.4 mM S-2288 at 25 °C in the same buffer. Essentially the same procedure was used for measurements of the Zn^{2+} concentration dependence of FVIIa binding to immobilization $TF_{1–219}$. In this case, the wells were incubated with 10 nM FVIIa in the presence of various concentrations (0–1 mM) of $ZnCl_2$. Control experiments with immobilization of 1 μg/mL bovine serum albumin showed no measurable binding of FVIIa.

Zn^{2+} binding measured by equilibrium dialysis

One hundred and fifty microliters of a 4 mg/mL solution of des(1–44)–FVIIa was placed inside a Slide-A-Lyzer 10K dialysis cassette (Pierce, Rockford, Illinois) and dialyzed against 200 mL of 50 mM HEPES, pH 7.5, containing 0.1 M NaCl and 20–500 μM $ZnCl_2$, for 16 h at 4 °C in the absence or presence of 5 mM $CaCl_2$. The concentration of Zn^{2+} in the inner and outer solutions was then measured by atomic absorption spectroscopy and the concentration of des(1–44)–FVIIa in the cassette was measured by spectrophotometry using a molar extinction coefficient at 280 nm of 56,300 cm^{-1}. The difference in zinc concentration between the inner and outer solutions, which represents zinc ions bound to des(1–44)–FVIIa, was divided by the protein concentration to obtain the number of zinc equivalents bound.

FFR-chloromethyl ketone alkylation and carbamylation of FVIIa

FVIIa (1 μM) was incubated with 6 μM FFR-chloromethyl ketone, or FVIIa/TF (40 nM/200 nM) was incubated with 120 nM FFR-chloromethyl ketone at 25 °C in 50 mM HEPES, 100 mM NaCl, 1 mM $CaCl_2$, 0.02% Tween 20, pH 7.4, in the presence or absence of 0.2 mM $ZnCl_2$. Twenty-five microliter samples were withdrawn at various times and added to 225 μL of 0.4 mM S-2288 in the same buffer. Residual activity was measured by the increase in absorbance at 405 nm. FVIIa (1 μM) or FVIIa/TF (200 nM/1 μM) was incubated with 0.2 M KNCO at 25 °C in 50 mM HEPES, 100 mM NaCl, 1 mM $CaCl_2$, 0.02% Tween 20, pH 7.4, in the presence or absence of 0.2 mM $ZnCl_2$. Samples (25 μL) were withdrawn at various times and added to 225 μL of 50 mM HEPES, pH 7.4, containing 100 mM NaCl, 5 mM $CaCl_2$, 0.1 mM EDTA, 0.02% Tween 20, and 0.4 mM S-2288. Residual activity was measured as in the above alkylation experiment.

Identification of putative Zn^{2+}-binding sites by molecular modeling

The X-ray structure of des(1–44)–FVIIa (Protein Data Bank (PDB) entry code: 1dan) was probed as described by Goodford (1985) using the Grid program (Molecular Discovery Ltd., Oxford, United

Kingdom). This program applies a force field parameterized for proteins. Identification of high-affinity interaction sites was based on calculations of the interaction energy between the protein and the probe in question. The sites of lowest interaction energy were visualization in Quanta (Molecular Simulations Inc., San Diego, California) and analyzed. One probe for calcium ions and one for zinc ions were applied. After guided placement of Zn^{2+} by the Grid calculations, the potential binding sites were further explored by refinement of the environment by means of the molecular modeling package Charmm (Brooks et al., 1983). The structures (considering all atoms within a radius of 10 Å from the zinc ion) were refined using a combination of steepest descent and conjugated gradient energy minimization methods. A distance-dependent dielectric constant of 1 was applied to compensate for the absence of solvent in the model.

Acknowledgments

We thank Elke Gottfriedsen, Annette Danielsen, and Anette Østergaard for expert technical assistance.

References

Banner DW, D'Arcy A, Chène C, Winkler FK, Guha A, Konigsberg WH, Nemerson Y, Kirchhofer D. 1996. The crystal structure of the complex of blood coagulation factor VIIa with soluble tissue factor. *Nature 380*:41–46.

Bernardo MM, Day DE, Olson ST, Halvorson HR, Shore JD. 1993a. Surface-independent acceleration of factor XII activation by zinc ions: II. Direct binding and fluorescence studies. *J Biol Chem 268*:12477–12483.

Bernardo MM, Day DE, Olson ST, Shore JD. 1993b. Surface-independent acceleration of factor XII activation by zinc ions: I. Kinetic characterization of the metal ion rate enhancement. *J Biol Chem 268*:12468–12476.

Brooks BR, Bruccolleri RE, Olafson BD, States DJ, Swaminathan S, Karplus M. 1983. CHARMM: A program for molecular energy minimization, and dynamics calculations. *J Comput Chem 4*:187–217.

Dickinson CD, Kelly CR, Ruf W. 1996. Identification of surface residues mediating tissue factor binding and catalytic function of the serine protease factor VIIa. *Proc Natl Acad Sci USA 93*:14379–14384.

Dickinson CD, Ruf W. 1997. Active site modification of factor VIIa affects interactions of the protease domain with tissue factor. *J Biol Chem 272*:19875–19879.

Du ZJ, Regier DA, Desrosiers RC. 1995. Improved recombinant PCR mutagenesis procedure that uses alkaline-denatured plasmid template. *Biotechniques 18*:376–378.

Freskgård P-O, Olsen OH, Persson E. 1996. Structural changes in factor VIIa induced by Ca^{2+} and tissue factor studied using circular dichroism spectroscopy. *Protein Sci 5*:1531–1540.

Freskgård P-O, Petersen LC, Gabriel DA, Li X, Persson E. 1998. Conformational stability of factor VIIa: Biophysical studies of thermal and guanidine hydrochloride-induced denaturation. *Biochemistry 37*:7203–7212.

Goodford PJ. 1985. A computational procedure for determining energetically favorable binding sites on biologically important macromolecules. *J Med Chem 28*:849–857.

Gordon PR, Woodruff CW, Anderson HL, O'Dell BL. 1982. Effects of acute zinc deprivation on plasma zinc and platelet aggregation in adult males. *Am J Clin Nutr 35*:113–119.

Gorodetsky R, Mou X, Blankenfeld A, Marx G. 1993. Platelet multi-element composition, lability and subcellular location. *Am J Hematol 42*:278–283.

Head DM, Matthews ITW, Tones MA. 1997. Effect of divalent ions on the binding of tissue factor and activated factor VII. *Thromb Res 85*:327–339.

Higashi S, Iwanaga S. 1998. Molecular interaction between factor VII and tissue factor. *Int J Hematol 67*:229–241.

Higashi S, Matsumoto N, Iwanaga S. 1996. Molecular mechanism of tissue factor-mediated acceleration of factor VIIa activity. *J Biol Chem 271*:26569–26574.

Higashi S, Nishimura H, Aita K, Iwanaga S. 1994. Identification of regions of bovine factor VII essential for binding to tissue factor. *J Biol Chem 269*:18891–18898.

Higashi S, Nishimura H, Fujii S, Takada K, Iwanaga S. 1992. Tissue factor potentiates the factor VIIa-catalyzed hydrolysis of an ester substrate. *J Biol Chem 267*:17990–17996.

Huber R, Bode W. 1978. Structural basis of the activation and action of trypsin. *Acc Chem Res 11*:114–122.

Libscomb WN, Strater N. 1996. Recent advances in zinc enzymology. *Chem Rev 96*:2375–2433.

Miyata T, Funatsu A, Kato H. 1995. Chemical cross-linking of activated coagulation factor VII with soluble tissue factor: Calcium ions are not essential for full activity of the factor VIIa-tissue factor complex after complex formation. *J Biochem 117*:836–844.

Nicolaisen EM, Petersen LC, Thim L, Jacobsen JK, Christensen M, Hedner U. 1992. Generation of Gla-domainless FVIIa by cathepsin G-mediated cleavage. *FEBS Lett 306*:157–160.

Pedersen AH, Lund-Hansen T, Komiyama Y, Petersen LC, Oestergård P, Kisiel W. 1991. Inhibition of recombinant human blood coagulation factor VIIa amidolytic and proteolytic activity by zinc ions. *Thromb Haemostas 65*:528–534.

Pedersen AH, Nordfang O, Norris F, Wiberg FC, Christensen PM, Moeller KB, Meidahl-Pedersen J, Beck TC, Norris K, Hedner U, Kisiel W. 1990. Recombinant human extrinsic pathway inhibitor. *J Biol Chem 265*:16786–16793.

Persson E, Nielsen LS. 1996. Site-directed mutagenesis but not γ-carboxylation of Glu-35 in factor VIIa affects the association with tissue factor. *FEBS Lett 385*:241–243.

Petersen LC, Persson E, Freskgård P-O. 1999. Thermal effects on an enzymatically latent conformation of coagulation factor VIIa. *Eur J Biochem 261*:124–129.

Petersen LC, Schiødt J, Christensen U. 1994. Involvement of hydrophobic stack residues 39–44 of coagulation factor VIIa in its interaction with tissue factor. *FEBS Lett 347*:73–79.

Pike ACW, Brzozowski AM, Roberts SM, Olsen OH, Persson E. 1999. Structure of human factor VIIa and its implications for the triggering of blood coagulation. *Proc Natl Acad Sci USA 96*:8925–8930.

Ruf W, Dickinson CD. 1998. Allosteric regulation of the cofactor-dependent serine protease coagulation factor VIIa. *Trends Cardiovasc Med 8*:350–356.

Schousboe I. 1990. The inositol-phospholipid-accelerated activation of prekallikrein by activated factor XII at physiological ionic strength zinc ions and high-Mr kininogen. *Eur J Biochem 193*:495–499.

Shimada T, Kato H, Iwanaga S. 1987. Accelerating effect of zinc ions on the surface-mediated activation of factor XII and prekallikrein. *J Biochem 102*:913–921.

Shobe J, Dickinson CD, Ruf W. 1999. Regulation of the catalytic function of coagulation factor VIIa by a conformational linkage of surface residue Glu 154 to the active site. *Biochemistry 38*:2745–2751.

Shore JD, Day DE, Bock PE, Olson ST. 1987. Acceleration of surface-dependent autocatalytic activation of blood coagulation factor XII by divalent metal ions. *Biochemistry 26*:2250–2258.

Sørensen BB, Persson E, Freskgård P-O, Kjalke M, Ezban M, Williams T, Rao LVM. 1997. Incorporation of an active site inhibitor in factor VIIa alters the affinity for tissue factor. *J Biol Chem 272*:11863–11868.

Thim L, Bjørn SE, Christensen M, Nicolaisen EM, Lund-Hansen T, Pedersen AH, Hedner U. 1988. Amino acid sequence and posttranslational modifications of human factor VIIa from plasma and transfected baby hamster kidney cells. *Biochemistry 27*:7785–7793.

Wildgoose P, Foster D, Schiødt J, Wiberg FC, Birktoft JJ, Petersen LC. 1993. Identification of a calcium site in the protease domain of human blood coagulation factor VII: Evidence for its role in factor VII-tissue factor interaction. *Biochemistry 32*:114–119.

Zhang E, St Charles R, Tulinsky A. 1999. Structure of extracellular tissue factor complexed with factor VIIa inhibited with a BPTI mutant. *J Mol Biol 285*:2089–2104.